Brownian Dynamics Simulations of Model Near-Hard-Sphere Suspensions

D. M. Heyes[a]; A. C. Branka[b]

[a] Department of Chemistry, University of Surrey, Guildford [b] Instytut Fizyki Molekularnej, Polskiej Akademii Nauk, Poznan, Poland

PLEASE SCROLL DOWN FOR ARTICLE

BROWNIAN DYNAMICS SIMULATIONS OF MODEL NEAR-HARD-SPHERE SUSPENSIONS

D. M. HEYES and A. C. BRANKA*

Department of Chemistry, University of Surrey, Guildford, GU2 5XH

Brownian dynamics simulations of near-hard sphere (r^{-24} potential particles) have been carried out for model colloidal systems using a free-draining model for the hydrodynamic interactions. The phase volume of solids considered is in excess of 50%. We investigated the N-dependence of the shear thinning curves and found that the rheology of $N = 108$ and $N = 256$ systems were statistically indistinguishable. We demonstrated that the shear induced ordering of the particles does not develop until the extent of shear thinning is nearly complete (i.e., as the second newtonian plateau is approached). We also report the effects of shear flow on the cartesian components of the pressure tensor and the long-time self-diffusion coefficients. This analysis suggests that all the thermodynamic and transport properties lose the x, y and z direction degeneracy, present at equilibrium under the non-equilibrium conditions established at high shear rates.

KEY WORDS: Colloidal systems, hydrodynamic interactions.

1 INTRODUCTION

The effects of high shear rates on the viscosity of molecular liquids and dense colloidal suspensions have been the subject of numerous experimental and computer simulation[1–16] studies over the years. Both light[17] and neutron scattering[18] experimental studies have given evidence of a shear-induced ordering of the colloidal particles in all three cartesian directions (the shear flow direction, the shear gradient direction and the vorticity direction). The picture from experiment as to what shear-induced ordering takes place close to the liquid-solid phase boundary of the colloidal system, is still not fully clarified and probably depends somewhat on the stabilisation mechanism of the colloidal particles (e.g., steric or charge stabilisation). The picture that is building up is that the fluid densifies along the vorticity direction (perpendicular to the flow plane) either as layers in the flow-vorticity plane or as "strings" of particles flowing down "tubes" along the flow direction. The density of particles along the flow direction progressively decreases as shear rate increases. There is a corresponding densification of particles along the shear gradient and vorticity directions. From simulations it is not yet possible to be definitive about when the

* Permanent address: Instytut Fizyki Molekularnej, Polskiej Akademii Nauk, Smoluchowskiego 17/19, 60-179 Poznan, Poland.

strings or layers appear because computational limitations have restricted the size of the simulation cell. We have not yet been able to investigate very large systems and the precise pattern could be system size dependent.

Another related issue is the symmetry of the "lattice" that forms. The lattice of particles formed by the flowing colloidal particles must fit in a simulation cell (usually cubic periodic). As there is a triangular component to the super-lattice there is a geometrical mismatch between the lattice which the fluid would like to form into and the periodic lattice of the simulation cell. Cook and Wilemski[19,20] have recently performed a study of this aspect of the simulations. At high shear rates, the system structure and the excess viscosity can vary erratically with system size.

At high solids volume fractions the hydrodynamic interactions between the particles are multi-body and are a formidable problem to solve for isolated configurations of colloidal particles. This would have to be performed at every time step in the simulation. The lack of any realistic treatment of many-body hydrodynamics in current codes also makes a comparison with experiment on hard-sphere colloids somewhat ambiguous at present. Nevertheless the simulations performed to date do show ordering not inconsistent with the experimental data.[17,18]

In the present work, we report the results of brownian dynamics simulations of model near-hard sphere colloidal suspensions. We investigate the change in structure of the model dispersion with shear rate and correlate this with the change in viscosity, normal pressure components and long-time self-diffusion coefficients that take place concurrently. We also investigate the system size dependence of the physical properties, for the limited number of N-values we can at present consider.

2   THE MODEL

The colloid particles interacted through a soft-sphere interaction,

$$\phi(r) = \epsilon(\sigma/r)^{24}, \tag{1}$$

where σ is the equivalent hard-core diameter of the colloid molecule and r is the centre-to-centre separation between the two model particles. This interaction mimics a sterically stabilised colloidal particle. The interaction is sufficiently hard to represent a hard-sphere for many purposes, without being too hard to cause algorithmic problems in the continuous potential particle update scheme. In these simulations we generated the positions of model colloidal particles subjected to a laminar shear flow, $\dot{\gamma} = \partial v_x/\partial y$. The molecular configurations were generated at fixed time intervals, h, using a Brownian Dynamics, BD, technique appropriate to large particle in a suspending medium. First we will describe the basics of BD and then the method of including the shear flow.

Let $\underline{F}$ be the force between the colloidal particles, obtained as usual from the potential (Eq. (1)). There are other forces arising from the interaction of the colloidal particle with the solvent. The Strict Langevin BD method employed here,[8] treats the suspending medium on two independent levels. The background fluid acts to dampen

out the velocities of the colloidal particles. The force on the particles by the solvent opposes the velocity through a friction coefficient, β. The discrete nature of the solvent is represented by a random force, $\underline{R}$ acting upon the colloidal particles. The value of the random force on each particle changes with time in order to represent the **net** effect of the collisions of the solvent molecules on the colloidal particle. In each time interval there is an imbalance on either side of the colloidal particle, leading to a net 'force, $\underline{R}$. This represents the net effect of the suspending medium over a fixed time interval (i.e., h). The acceleration of the colloidal particles is therefore,

$$\ddot{\underline{r}} = \underline{F}/m + \underline{R}/m - \beta\dot{\underline{r}}, \tag{2}$$

where r is the position of an arbitrary macromolecule,

$$r_x(t + h) = r_x(t) + (F_x(t) + R_x(t, h))h/m\beta + \dot{\gamma}R_y, \tag{3}$$

$$r_y(t + h) = r_y(t) + (F_y(t) + R_y(t, h))h/m\beta, \tag{4}$$

$$r_z(t + h) = r_z(t) + (F_z(t) + R_z(t, h))h/m\beta \tag{5}$$

We have assumed that the mass of each particle, i, is proportional to σ^3. The shear rates are made dimensionless by scaling according to a characteristic relaxation time, τ, the time it takes a colloidal particle at infinite dilution to (on average) diffuse half its diameter, σ.

$$\tau_r = 3\pi\sigma^3\eta_0/4k_BT, \tag{6}$$

The Peclet number is $Pe = \dot{\gamma}\tau_r/2$. The viscosity of the solvent is η_0. We computed the pressure tensor, P,

$$P_{\alpha\beta} = \frac{1}{V}\sum_{i=1}^{N-1}\sum_{j}^{N}(r_{\alpha ij}r_{\beta ij}/r_{ij})\phi'_{ij}, \tag{7}$$

where V is the volume of the simulation cell containing N model colloid particles. The number density of particles, ρ is defined according to $\rho = N\sigma^3/V$, and ϕ_{ij} is the pair potential between i and j. The viscosity is defined from the xy component of the pressure tensor, P_{xy}. Time averaged over a simulation at a fixed shear rate, we have,

$$\eta = -P_{xy}/\dot{\gamma}, \tag{8}$$

The viscosities are conventionally non-dimensionalised by the viscosity of the solvent, leading to the definition of the relative viscosity, $\eta_r = \eta/\eta_0$. The infinite dilution self-diffusion coefficient is defined according to,

$$D_0 = \sigma^2/8\tau_r, \tag{9}$$

Over the complete volume fraction range the following analytical expressions fit the relative viscosity data within experimental uncertainty,[23]

$$\eta_r(Pe \rightarrow 0) = (1 - \phi/0.63)^{-2}, \tag{10}$$

and,

$$\eta_r(Pe \rightarrow \infty) = (1 - \phi/0.71)^{-2}, \tag{11}$$

where, $\phi = \pi N\sigma^3/6V$. The underlying equilibrium thermodynamics of the colloidal fluid is determined very closely by the hard-sphere equation of state. The equation of state of the hard-sphere fluid is well represented by,

$$PV/Nk_BT = 1 + b\rho/(1 - \rho/\rho_0)^2, \tag{12}$$

where $b = 2\pi\sigma^3/3$ and $\rho_0 = 1.605\sigma^{-3}$.[22]

3.   RESULTS AND DISCUSSION

In Figure 1(a) we show the shear rate dependence of the relative viscosity for two volume fractions, $\phi = 0.5$ and $\phi = 0.55$. Both of these are in the "glassy" region of
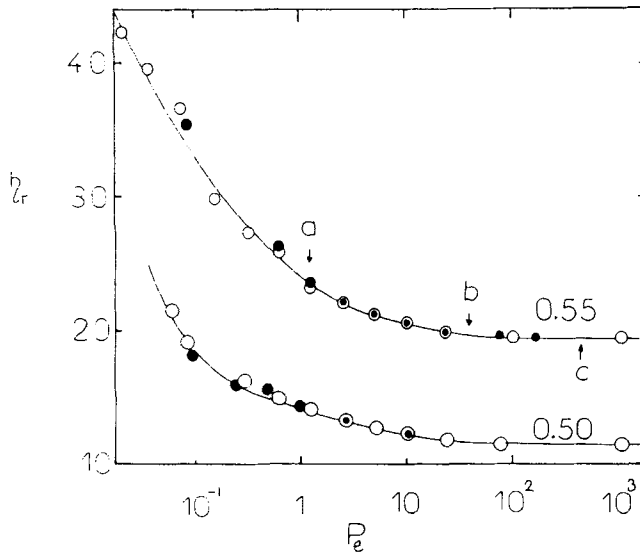
Figure 1   The relative viscosity of the model dispersions on varying Pe. Two volume fractions are considered. These are $\phi = 0.5$ and $\phi = 0.55$, indicated on the figure. The data from two sets of simulations are considered with $N = 256$ (open circles) and $N = 108$ (closed circles).
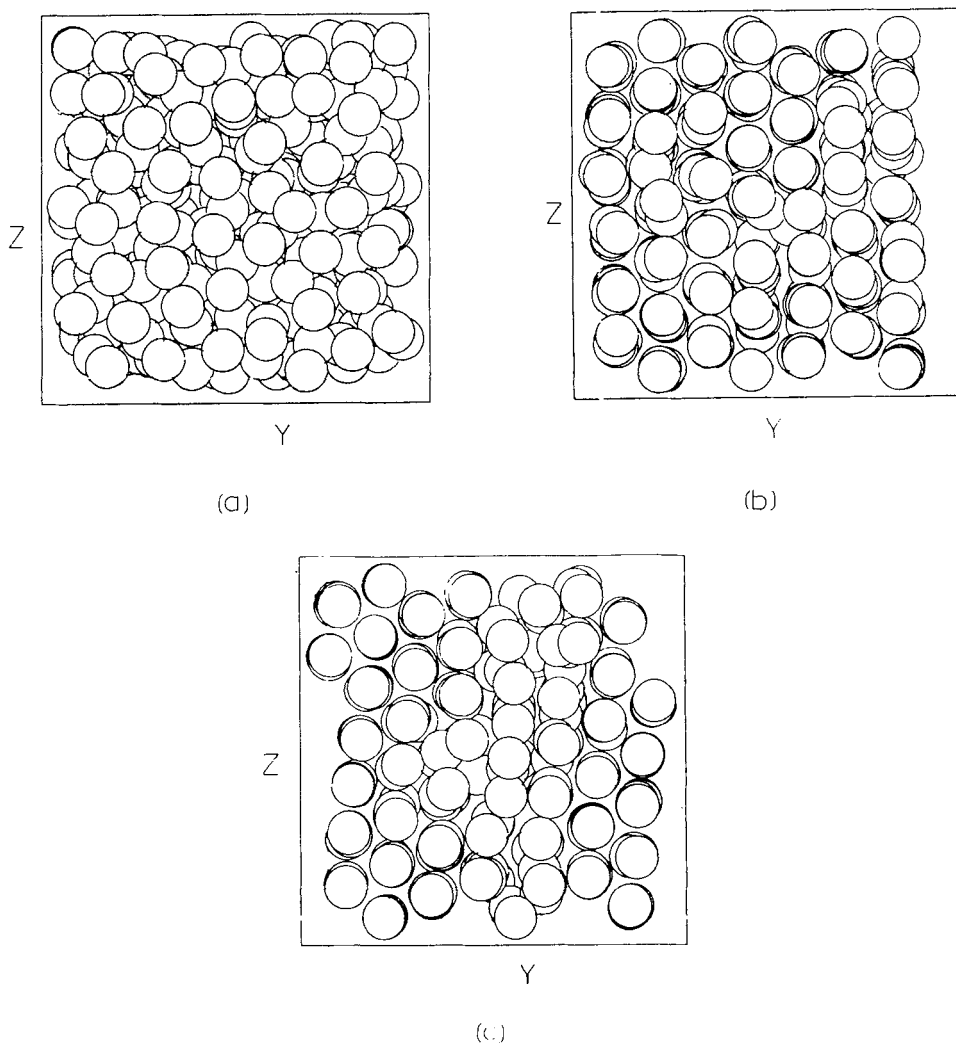
Figure 2 Perspective images of instantaneous configurations taken from the brownian dynamics simulations. The view is in the gradient (y), vorticity (z) direction. Three Peclet numbers are considered. (a) $Pe = 1.3$, (b) $Pe = 41.0$ and (c) $Pe = 328$. The volume fraction is $\phi = 0.55$ and $N = 256$.

the hard-sphere phase diagram, but nevertheless are frequently studied experimentally. The newtonian viscosities for these states are, according to Eqs. (10) and (11), 21 and 62. The two curves appear to be extrapolating to limits at zero Peclet number not too dissimilar from these values. The statistical uncertainty at low shear rates hinders any more meaningful conclusion. Reassuringly, the viscosities obtained using two system sizes, $N = 108$ and $N = 256$ are within statistical uncertainty identical.

In the Figure 2 we show some examples of the structures formed by the model under flow. The spheres in the figures are the colloidal particles, shown with some measure of perspective. The plane viewed is the shear gradient-vorticity (yz) plane. Figure 2(a) shows the $\phi = 0.55$, $N = 256$ and $Pe = 1.3$ state (marked (a) in Figure 1). This is well within the shear thinning part of the rheogram for this colloidal system. It shows no obvious evidence for structural rearrangement due to shear. The same system at $Pe = 41$ presents a quite different arrangement of the spheres. There is clear evidence, in Figure 2(b), (marked (b) in Figure 1) of a reordering of the colloidal particles into "strings" flowing along the shear flow direction. In Figure 2(c) (marked (c) in Figure 1) this is still present. Therefore shear thinning is evident even without any major structural change in the fluid. At the approach of the levelling off of the relative viscosity at high Pe, the so-called second newtonian plateau, we see the development of long range order.

The cartesian components of the compressibility factor are given in Figure 3. The pressure components increase from the equilibrium value to a local maximum just prior to the onset of the string phase. The pressure components decrease during this phase-change before increasing further. Even though the string phase appears to
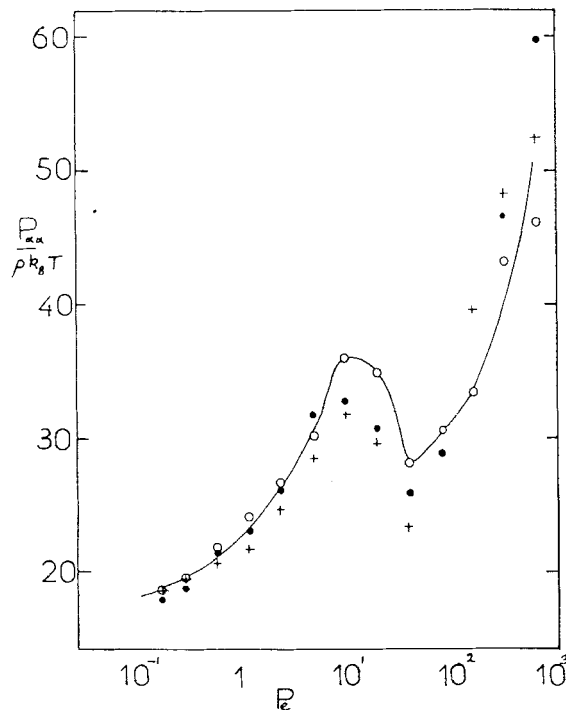
Figure 3   The cartesian component of the pressure tensor $P_{\alpha\alpha}/\rho k_B T$ versus Pe. $N = 256$ and $\phi = 0.55$. $\alpha = x$, open circle; $\alpha = y$, filled circle; $\alpha = z$, cross.
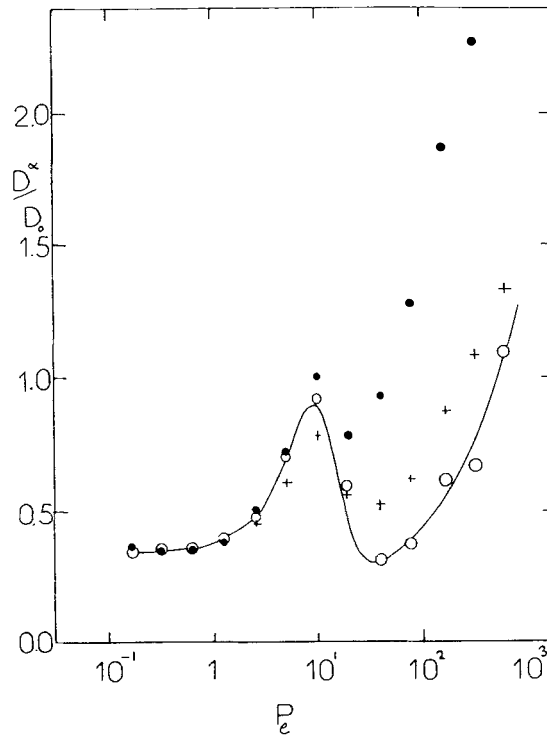
Figure 4 The cartesian components of the long-time self-diffusion coefficients, D_α/D_0 versus Pe. $N = 256$ and $\phi = 0.55$. $\alpha = x$, open circle; $\alpha = y$, filled circle; $\alpha = z$, cross.

change a little in appearance, there is still a continual evolution in the pressure within this phase as shear rate increases.

The self-diffusion coefficients of sheared fluids are known to vary with the magnitude of the shear rate.[24] In Figure 4, we show the long time self-diffusion coefficients (normalised by D_0) as a function of shear rate for the $\phi = 0.55$ states. The component diffusion coefficients, D_α, were evaluated via the mean-square displacements of the particles, eliminating the displacement due to the shear flow itself.[12] The appearance of the string phase again causes a temporary halt to the increase in this property with shear rate. Note that the three cartesian component self-diffusion coefficients become increasingly different as shear rate increase, particularly within the string phase.

4 CONCLUSIONS

In this note we have continued our investigations of the effect of large shear rates on colloidal dispersions, using the brownian dynamics technique. The main new features of this study, are that we have investigated the N-dependence of the relative

viscosity at very high solids volume fractions. The relative viscosity proved to be essentially independent of N between $N = 108$ and $N = 256$. We have also introduced a new form of visualisation of the colloidal model which is an improvement on the strictly 2-dimensional representations used in previous reports of this programme of work. We have also given further evidence that the thermodynamic and transport properties lose the x, y and z direction degeneracy at high shear rates. They also manifest strong variations in behaviour during the transition from the amorphous (low shear rate) states to the ordered (high shear rate) states.

References

1. D. M. Heyes, J. J. Kim, C. J. Montrose and T. A. Litovitz, *J. Chem. Phys.*, **73**, 3987 (1980).
2. S. M. Rekhson, D. M. Heyes, C. J. Montrose and T. A. Litovitz, *J. of Non-Cryst. Solids* **38 & 39**, 403 (1980).
3. D. M. Heyes, C. J. Montrose and T. A. Litovitz, *J. Chem. Soc. Faraday Trans. II*, **79**, 611 (1983).
4. D. M. Heyes, *Physica A* **133**, 473 (1985).
5. D. M. Heyes, G. P. Morriss and D. J. Evans, *J. Chem. Phys.* **83**, 4760 (1985).
6. D. M. Heyes, *J. Non. Newt. Fl. Mech.*, **21**, 137 (1986).
7. D. M. Heyes, *J. Chem. Phys.* **85**, 997 (1986).
8. D. M. Heyes, *Chem. Phys. Lett.* **127**, 515 (1986).
9. D. M. Heyes, *J. Chem. Soc. Faraday Trans. II* **82**, 1365 (1986).
10. D. M. Heyes, *Chem. Phys.* **47**, 109 (1986).
11. D. M. Heyes, *Mol. Phys.* **57**, 1265 (1986).
12. D. M. Heyes, *J. Non-Newt. Fl. Mech.* **27**, 47 (1988).
13. D. M. Heyes and J. R. Melrose, *Mol. Sim.* **2**, 281 (1988).
14. D. M. Heyes, *Comp. Phys. Rep.* **8**, 71 (1988).
15. D. M. Heyes, *Phys. Lett. A* **132**, 399 (1988).
16. M. W. Evans and D. M. Heyes, *Mol. Phys.* **65**, 1441 (1988).
17. B. J. Ackerson, *J. Rheol.* **34**, 553 (1990).
18. R. H. Ottewill and A. R. Rennie, *Int. J. Multiphase Flow*, **16**, 681 (1990).
19. R. Cook and G. Wilemski, *J. Phys. Chem.* **96**, 4023 (1992).
20. G. Wilemski, *J. Stat. Phys.* **62**, 1239 (1991).
21. B. H. A. A. van den Brule and R. J. J. Jongschapp, *J. Stat. Phys.* **62**, 1225 (1991).
22. D. M. Heyes and P. J. Aston, *J. Chem. Phys.* **97**, 5738 (1992).
23. W. B. Russel, D. A. Saville and W. R. Schowalter, "Colloidal Dispersions", Cambridge Univ. Press, 1989, p. 466.
24. S. Sarman, D. J. Evans and A. Baranyai, *Phys. Rev. A* **46**, 893 (1992).